

# Role of the Pauli principle in collective-model coupled-channels calculations

L. Canton<sup>(1),\*</sup> G. Pisent<sup>(1),†</sup> J. P. Svenne<sup>(2),‡</sup> D. van der Knijff<sup>(3),§</sup> K. Amos<sup>(4),¶</sup> and S. Karataglidis<sup>(4)\*\*</sup>

<sup>(1)</sup> *Istituto Nazionale di Fisica Nucleare, Sezione di Padova,  
e Dipartimento di Fisica dell'Università di Padova, via Marzolo 8, Padova I-35131, Italia*

<sup>(2)</sup> *Department of Physics and Astronomy, University of Manitoba,  
and Winnipeg Institute for Theoretical Physics, Winnipeg, Manitoba, Canada R3T 2N2*

<sup>(3)</sup> *Advanced Research Computing, Information Division,  
University of Melbourne, Victoria 3010, Australia and*

<sup>(4)</sup> *School of Physics, University of Melbourne, Victoria 3010, Australia*  
(Dated: July 10, 2018)

A multi-channel algebraic scattering theory, to find solutions of coupled-channel scattering problems with interactions determined by collective models, has been structured to ensure that the Pauli principle is not violated. By tracking the results in the zero coupling limit, a correct interpretation of the sub-threshold and resonant spectra of the compound system can be made. As an example, the neutron-<sup>12</sup>C system is studied defining properties of <sup>13</sup>C to 10 MeV excitation. Accounting for the Pauli principle in collective coupled-channels models is crucial to the outcome.

PACS numbers: 24.10.-i;25.40.Dn;25.40.Ny;28.20.Cz

At energies above 25 MeV, by using optical potentials formed by full folding effective two-nucleon interactions with microscopic (nucleon based) descriptions of the target structure, the importance of treating the Pauli principle has been well established [1]. However, in the domain of low-energy nucleon scattering for which an explicit coupled-channels theory of scattering is essential, the significance of Pauli exclusion effects has not been well defined. Many coupled-channels codes are available, some of which perform phenomenological collective-model calculations searching on parameter values of the chosen function forms to find a best fit to experimental data. But while it has long been known that any such models violate the Pauli principle [2, 3], quantification of that violation is lacking.

To study the effects of the Pauli principle in a macroscopic (collective model) approach is not a trivial task. In a recent publication [4], the orthogonalizing pseudo-potential (OPP) method [5, 6] was generalized to treat this problem. That was a small though important part of the full theoretical framework of the multi-channel algebraic scattering (MCAS) theory of scattering [4]. Therein the OPP was used in finding the spectra, bound and resonance properties, of <sup>13</sup>C. However, implications of the role of the Pauli principle in collective model coupled-channel calculations arising from the use of the OPP was not discussed. Such is a purpose of this letter. Another is that the method could be pertinent for any study requiring coupled channel solutions of quantal systems involving fermions. As the example, we study the effects introduced by the Pauli principle in collective, geometrical-type, models for low-energy nucleon-nucleus processes that can be characterized from the spectrum

of the compound nucleus. That spectrum includes the states that lie below the nucleon-nucleus threshold and in the continuum as revealed by the narrow and broad resonances that lie upon a smooth but energy dependent background of the elastic scattering cross section. This can be done in a systematic and self-consistent way since the MCAS approach facilitates such a determination of the sub-threshold bound states and resonances of the compound nucleus. This theory, with which one solves the coupled-channel Lippmann-Schwinger (LS) equations for the nucleon-nucleus system considered, is built upon Sturmian expansions of an interaction matrix of potential functions.

The MCAS method has been developed in momentum space and the starting matrix of potentials may be formed by folding effective two-nucleon interactions with one-body density matrices of the target (studies in progress) or, as is more common, from a collective model description of the target states and excitations. As in that recent publication [4], we have used a rotational collective-model representation with deformation taken to second order. We chose Woods-Saxon functions and their various derivatives to be the form factors for all components each with characteristic operators of diverse type. The interactions were allowed to depend on parity as well. With such a characterization, we were able to describe all important aspects, at positive and negative energies, in the neutron-<sup>12</sup>C system.

With the MCAS approach and a collective model prescription for the starting matrix of potentials, the OPP is used in the process by which the Sturmians are specified. The OPP inclusion ensures that all Sturmians in the (finite) set selected as the basis of expansion of the matrix

of potentials contain few or no components equivalent to the external nucleon being placed in an already densely occupied orbit. That scheme is an approximation as we discuss later by assessing the spectra of  $^{12,13}\text{C}$  and the single neutron spectroscopic amplitudes that link them using information obtained from large space no-core shell model calculations. But it is a good approximation.

The role of the Pauli principle is studied by comparing results found with and without using the OPP scheme to select the sturmians that form the expansion set. Note that the actual matrix of potentials is the same throughout though extra information on single nucleon plus a core nucleus state underlying each sub-threshold bound and resonance in the compound system has been obtained by taking the zero deformation limit.

Full details of the MCAS scheme have been published [4] and the reader is referred there for those, as well as for specifics of the notation we use herein. In momentum space for potential matrices  $V_{cc'}(p, q)$ , one seeks the solution of coupled LS equations [see Eq. (1) in Ref. [4]], which involve both open and closed channel contributions. With incident energy  $E$ , the channel wave numbers for the open and closed channels are  $k_c$  and  $h_c$  respectively. Solutions of those LS equations are sought using expansions of the potential matrix elements in (finite) sums of energy-independent separable terms,

$$V_{cc'}(p, q) \sim \sum_{n=1}^N \hat{\chi}_{cn}(p) \eta_n^{-1} \hat{\chi}_{c'n}(q), \quad (1)$$

where  $\hat{\chi}_{c'n}(q)$  are the Fourier-Bessel transforms of the selected sturmians whose eigenvalues are  $\eta_n$ . To predict observables one requires the multichannel  $S$ -matrix. In terms of the multi-channel  $T$ -matrix, that has closed algebraic form

$$\begin{aligned} S_{cc'} &= \delta_{cc'} - i\pi\mu\sqrt{k_c k_{c'}} T_{cc'} \\ T_{cc'} &= \sum_{n, n'=1}^N \hat{\chi}_{cn}(k_c) ([\boldsymbol{\eta} - \mathbf{G}_0]^{-1})_{nn'} \hat{\chi}_{c'n'}(k_{c'}), \end{aligned} \quad (2)$$

where now  $c, c'$  refer to open channels only. In this representation,  $\mathbf{G}_0$  and  $\boldsymbol{\eta}$  have matrix elements

$$\begin{aligned} [\mathbf{G}_0]_{nn'} &= \mu \left[ \sum_c^{\text{open}} \int_0^\infty \hat{\chi}_{cn}(x) \frac{x^2}{k_c^2 - x^2 + i\varepsilon} \hat{\chi}_{c'n'}(x) dx \right. \\ &\quad \left. - \sum_c^{\text{closed}} \int_0^\infty \hat{\chi}_{cn}(x) \frac{x^2}{h_c^2 + x^2} \hat{\chi}_{c'n'}(x) dx \right], \\ [\boldsymbol{\eta}]_{nn'} &= \eta_n \delta_{nn'}. \end{aligned} \quad (3)$$

The bound states of the compound system are defined by the zeros of the matrix determinant when the energy  $E$  is negative, and so link to the zeros of  $\{|\boldsymbol{\eta} - \mathbf{G}_0|\}$  when all channels in Eq. (3) are closed.

As noted above the sturmians are solutions of homogeneous Schrödinger equations for the matrix of potentials.

TABLE I: Shell occupancies of protons (or neutrons) in states of  $^{12}\text{C}$ .

orbit	$0_1^+$	$2_1^+$	$0_2^+$
$0s_{\frac{1}{2}}$	1.963	1.962	1.968
$0p_{\frac{3}{2}}$	3.054	2.858	3.075
$0p_{\frac{1}{2}}$	0.842	1.028	0.804
higher orbits	0.124	0.129	0.120

In coordinate space if those potentials are designated by local forms  $V_{cc'}(r)\delta(r - r')$ , the OPP method is to use sturmians that are solutions for nonlocal potentials

$$\mathcal{V}_{cc'}(r, r') = V_{cc'}(r)\delta(r - r') + \lambda A_c(r)A_{c'}(r')\delta_{cc'}, \quad (4)$$

where  $A(r)$  is the radial part of the single particle bound state wave function in channel  $c$  spanning the phase space excluded by the Pauli principle. The OPP method holds in the limit  $\lambda \rightarrow \infty$ , but use of  $\lambda = 100$  MeV suffices.

The spectrum of  $^{12}\text{C}$  also was calculated in the shell model using the program OXBASH [7] and with the MK3W interaction [8]. The positive parity states of  $^{12}\text{C}$  were calculated in a complete  $(0 + 2)\hbar\omega$  space using this interaction, while the negative parity states were calculated in a restricted  $(1 + 3)\hbar\omega$  space. In both calculations the same single particle basis of  $0s$  up to and including the  $0f1p$  shell was used. Hence the restriction from a full  $(1 + 3)\hbar\omega$  study is that we have not included the  $0g1d2s$  shell. With exceptions, most notably the super-deformed  $0_2^+$  state at 7.654 MeV and the known collective  $3^-$  state at 9.64 MeV, the calculated spectrum to 20 MeV excitation agrees well with observation [1]. So also do results of calculations [1] of elastic and inelastic scattering data (form factors from electron scattering and differential cross sections and analyzing powers from proton scattering) without the need for any *a posteriori* core polarization corrections.

Of interest here are the details of the low lying spectrum. First, in Table I, we list the nucleon shell occupancies in the three lowest states of  $^{12}\text{C}$ . Clearly the  $0s$ - and  $0p$ - shells have dense occupancy: essentially 4 nucleons filling the  $0s$  shell while there are almost 8 nucleons in the  $0p$  shell. Those eight nucleons are distributed between the sub-shells, so blocking the  $0p_{\frac{3}{2}}$  orbit as we do in using the OPP method is an approximation. Note also that the second excited state of  $^{12}\text{C}$ , the  $0_2^+$  (7.654 MeV) is well known to be a super-deformed  $3\alpha$  chain and, as such, a much larger space is needed for a good description. The lowest three  $0^+$  states in our shell model are the ground, at 12.25, and at 23.03 MeV. They are much more spread than measured energies and have structure

$$\begin{aligned} |^{12}\text{C} (0_1^+) \rangle &= 80.525\% |0\hbar\omega\rangle + 19.475\% |2\hbar\omega\rangle \\ |^{12}\text{C} (0_2^+) \rangle &= 78.213\% |0\hbar\omega\rangle + 21.786\% |2\hbar\omega\rangle \\ |^{12}\text{C} (0_3^+) \rangle &= 9.066\% |0\hbar\omega\rangle + 90.934\% |2\hbar\omega\rangle. \end{aligned}$$

TABLE II: Dominant components of shell model spectroscopic amplitudes. Energies in brackets are in MeV.

$^{13}\text{C}$			$^{12}\text{C}$			
			$0_1^+$	$2_1^+$	$0_2^+$	
$\frac{1}{2}^-$	(g.s.)	$0p_{\frac{1}{2}}$	-0.7285	$0p_{\frac{3}{2}}$	-1.0040	$0p_{\frac{1}{2}}$ -0.4738
$\frac{1}{2}^+$	(3.09)	$1s_{\frac{1}{2}}$	-0.9088	$0d_{\frac{5}{2}}$	-0.3162	$1s_{\frac{1}{2}}$ -0.0605
$\frac{3}{2}^-$	(3.68)	$0p_{\frac{3}{2}}$	0.4504	$0p_{\frac{3}{2}}$	-1.0040	$0p_{\frac{3}{2}}$ -0.3284
				$0f_{\frac{5}{2}}$	-0.8342	
$\frac{5}{2}^+$	(3.85)	$0d_{\frac{5}{2}}$	0.8129	$0d_{\frac{5}{2}}$	0.4799	$0d_{\frac{5}{2}}$ 0.0096
				$0d_{\frac{3}{2}}$	-0.1361	
				$1s_{\frac{1}{2}}$	0.0840	
$\frac{5}{2}^+$	(6.86)	$0d_{\frac{5}{2}}$	-0.2147	$0d_{\frac{5}{2}}$	0.5372	$0d_{\frac{5}{2}}$ -0.0102
				$0d_{\frac{3}{2}}$	-0.0907	
				$1s_{\frac{1}{2}}$	-0.7714	
$\frac{5}{2}^+$	(8.88)	$0d_{\frac{5}{2}}$	-0.0349	$0d_{\frac{5}{2}}$	-0.2568	$0d_{\frac{5}{2}}$ 0.2829
				$0d_{\frac{3}{2}}$	-0.2694	
				$1s_{\frac{1}{2}}$	-0.2391	

Notice that the first dominantly  $2\hbar\omega$  state lies at 23.03 MeV excitation; a calculated energy that can be expected to fall with the addition of higher  $\hbar\omega$  components. That has not been seen sufficiently at least to the  $4\hbar\omega$  level with an *ab initio* shell model [9]. So while the  $0_3^+$  state may be the one that is super-deformed, a convergence in energy will require a greatly increased space. But as the  $0_2^+$  state is not very important in the formation of resonances and bound states [4], use of our shell model should suffice for the comparisons we make. This may have more bearing on future results as we move to use a microscopic MCAS in which the matrices of interaction potentials will be formed using nucleon-based structure.

Next we consider how each state in the low excitation spectrum of  $^{13}\text{C}$  maps onto a single neutron added to any of the three selected states of  $^{12}\text{C}$ . The relevant one-body spectroscopic amplitudes for  $I^\pi \rightarrow J^{\pi'}$ ,

$$S_{j\frac{1}{2}} = \frac{1}{\sqrt{2(2J+1)}} \left\langle (^{13}\text{C}) J^{\pi'} \left\| \left\| a_{j,\frac{1}{2}}^\dagger \right\| \right\| (^{12}\text{C}) I_i^\pi \right\rangle, \quad (5)$$

are listed in Table II. The shell model calculations gave more values for addition of that neutron in higher shell states, but those spectroscopic amplitudes (not listed) all have magnitudes less than 0.1.

Results of calculations of the neutron- $^{12}\text{C}$  system reported previously [4], used the parameter values that are specified in Table III.

In Fig. 1, the results are compared with data, both elastic scattering cross sections as well as the spectrum of  $^{13}\text{C}$ . Therein it is clear that the three states of  $^{12}\text{C}$  suffice to deal with information to  $\sim 10$  MeV excitation

TABLE III: Parameter values of the base potential (in MeV).

	$V_0(\pi)$	$V_{\ell\ell}(\pi)$	$V_{\ell s}(\pi)$	$V_{Is}(\pi)$
$\pi = -$	-49.144	4.559	7.384	-4.770
$\pi = +$	-47.563	0.610	9.176	-0.052
Geometry	$R_0 = 3.09$ fm $a = 0.65$ fm $\beta_2 = -0.52$			

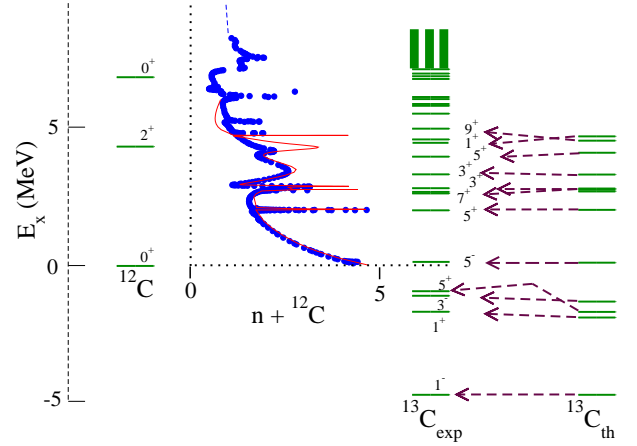


FIG. 1: The spectra of  $^{12,13}\text{C}$  and the elastic cross section (barn) for  $n+^{12}\text{C}$  system. The ENDF data (circles) [10] are compared with our full MCAS results (solid line). Note that the identification of the  $^{13}\text{C}$  states' spin-parities is  $2J^\pi$ .

in the compound with corroboration in the scattering of up to 5 MeV. Spin-parity assignments, bound state energies and resonance centroids, widths of the resonances, and the background scattering all are very well matched by the calculations. A most interesting feature is what occurs as the coupling tends to zero. In that limit, all of the compound resonances shrink to be bound states

TABLE IV: Pauli effects on sub-threshold and bound states in the continuum in the limit  $\beta_2 \rightarrow 0$  (with  $V_{ss} = 0$ ).

$J^\pi$	With Pauli	No Pauli	$n+^{12}\text{C}$
$\frac{1}{2}^+$	-	-26.57	$0s_{1/2} + 0_1^+$
$\frac{3}{2}^+, \frac{5}{2}^+$	-	-22.13	$0s_{1/2} + 2_1^+$
$\frac{1}{2}^+$	-	-18.91	$0s_{1/2} + 0_2^+$
$\frac{3}{2}^-$	-	-8.849	$0p_{3/2} + 0_1^+$
$\frac{1}{2}^-$	-4.685	-4.685	$0p_{1/2} + 0_1^+$
$\frac{1}{2}^-, \frac{3}{2}^-, \frac{5}{2}^-, \frac{7}{2}^-$	-	-4.410	$0p_{3/2} + 2_1^+$
$\frac{3}{2}^-$	-	-1.195	$0p_{1/2} + 0_2^+$
$\frac{1}{2}^+$	-0.837	-0.837	$1s_{1/2} + 0_1^+$
$\frac{3}{2}^-, \frac{5}{2}^-$	-0.246	-0.246	$0p_{1/2} + 2_1^+$
$\frac{5}{2}^+$	-0.171	-0.171	$0d_{5/2} + 0_1^+$
$\frac{1}{2}^-$	2.969	2.969	$0p_{1/2} + 0_2^+$
$\frac{3}{2}^+, \frac{5}{2}^+$	3.601	3.601	$1s_{1/2} + 2_1^+$
$\frac{1}{2}^+, \frac{3}{2}^+, \frac{5}{2}^+, \frac{7}{2}^+, \frac{9}{2}^+$	4.267	4.267	$0d_{5/2} + 2_1^+$

in the continuum. In this limit, calculations were made with the spin-spin interaction strengths set to zero, and so offsetting a splitting that is most evident with the two odd parity states built from coupling with a  $0p_{1/2}$  neutron. The results of these limit calculations are collected in Table IV. Therein the states are listed in the order from most bound to largest continuum energy whether they are real or spurious. The energies listed in columns 2 and 3 respectively were found in the zero deformation limit with and without the OPP treatment of Pauli blocking. In the last column we display what dominant character (neutron orbit coupled to state in  $^{12}\text{C}$ ) is found for each state in  $^{13}\text{C}$ . Disregarding the Pauli principle clearly gives many spurious states. However, notice that there are matching entries for every resonance state whether the Pauli principle is taken into account or not. That has led to the erroneous belief that a simple adjustment of parameter values is all that is needed to define scattering cross sections and that the Pauli principle effects are unimportant for scattering. Not only is that phenomenology not guaranteed to work in other cases but also the mixing of components caused by finite deformation is quite different when the Pauli principle is or is not satisfied. A calculation made ignoring the Pauli principle gives an incorrect description of all states.

The resonance centroids tend to three limits. The highest is at 4.267 MeV with five entries from  $\frac{1}{2}^+$  to  $\frac{9}{2}^+$  as is formed by attaching a  $0d_{5/2}$  neutron to the  $2^+$  state in  $^{12}\text{C}$ . The second is at 3.601 MeV having two entries which equate to a  $1s_{1/2}$  neutron coupled to the  $2^+$  state of the target. The third, the only odd parity resonance ascertained from these calculations within the range of energies to 5 MeV, is identified as a  $\frac{1}{2}^-$  resonance. It lies 7.65 MeV above the calculated value for the  $^{13}\text{C}$  ground state and can then be associated with binding a  $0p_{1/2}$  neutron to the second  $0^+$  state of  $^{12}\text{C}$ .

The bound states are less clear with regard to dominant particle coupling character. From shell model calculations, the  $\frac{1}{2}^-$  (ground state) and the  $\frac{3}{2}^-$  state are sizable mixtures of  $p$ -shell nucleon coupling to both the ground and  $2^+$  states in  $^{12}\text{C}$ . But the  $\frac{1}{2}^+$  and  $\frac{5}{2}^+$  bound states in  $^{13}\text{C}$  are dominantly formed respectively by a  $1s_{1/2}$  and a  $0d_{5/2}$  neutron coupled to the ground state of  $^{12}\text{C}$ . The energies found in the zero coupling limit support the inferences made above. Notably, the bound  $\frac{5}{2}^+$  tends to  $-0.171$  MeV in that limit, as  $4.267 - (-0.171) = 4.438$  MeV; the excitation energy of the  $2^+$  state in  $^{12}\text{C}$ . Likewise the doublet  $\frac{3}{2}^+, \frac{5}{2}^+$  tends to 3.601 MeV and as the bound state  $\frac{1}{2}^+$  tends to  $-0.837$  MeV in the zero coupling limit,  $3.601 - (-0.837) = 4.438$  MeV, the excitation energy of the  $2^+$  state in  $^{12}\text{C}$  once more. Finally the  $\frac{3}{2}^-$  and  $\frac{5}{2}^-$  states both are bound by  $-0.246$  MeV and so the energy gap of that pair from the  $\frac{1}{2}^-$  state ( $-4.685$  MeV),

is 4.439 MeV.

But deformation makes significant admixing of these nucleon plus core nucleus elements. Indeed it is this spurious mixing that is the most serious concern about calculations that do not take the Pauli principle into account. To reveal that, we have repeated the limit calculations excising the OPP effects and thereby solving the problem in a way equivalent to coordinate-space solutions of such coupled channels equations. That calculation clearly has given spurious states.

Summarizing, the MCAS approach has been used to evaluate (low-energy)  $n$ - $^{12}\text{C}$  elastic scattering and to characterize sub-threshold states of  $^{13}\text{C}$ . A collective model prescription with the three lowest states in the  $^{12}\text{C}$  spectrum was used. The results well match observed data but only when allowance for the influence of the Pauli principle was made. Without such allowance, many spurious states result. Most strikingly, the ground state of  $^{13}\text{C}$  then has the wrong spin-parity and a binding far in excess of the known value. But more disturbing is that when states may be matched (in energy and spin-parity) their underlying nucleon plus  $^{12}\text{C}$  compositions are wrong. By tracking results to the  $\beta_2 \rightarrow 0$  limit, the dominant parentage of each sub-threshold and resonant state in this system has been identified.

---

\* Electronic address: luciano.canton@pd.infn.it

† Electronic address: gualtieri.pisent@pd.infn.it

‡ Electronic address: svenne@physics.umanitoba.ca

§ Electronic address: dirk@unimelb.edu.au

¶ Electronic address: amos@physics.unimelb.edu.au

\*\* Electronic address: kara@physics.unimelb.edu.au

- [1] K. Amos, P. J. Dortmans, H. V. von Geramb, S. Karataglidis, and J. Raynal, *Adv. in Nucl. Phys.* **25**, 275 (2000).
- [2] C. Mahaux and H. A. Weidenmuller, *Shell model approach to nuclear reactions* (North-Holland, Amsterdam, 1969).
- [3] W. Greiner and J. A. Maruhn, *Nuclear models* (Springer-Verlag, Berlin, 1996).
- [4] K. Amos, L. Canton, G. Pisent, J. P. Svenne, and D. van der Knijff, *Nucl. Phys.* **A728**, 65 (2003).
- [5] V. Kukulin and V. Pomerantsev, *Ann. of Phys.* **111**, 330 (1978).
- [6] S. Saito, *Prog. Theor. Phys.* **41**, 705 (1969).
- [7] A. Etchegoyen, W. D. M. Rae, and N. S. Godwin, *OXBASH-MSU (the Oxford-Buenos-Aires-Michigan State University shell model code)*, *MSU version by B. A. Brown* (1986).
- [8] E. K. Warburton and D. J. Millener, *Phys. Rev. C* **39**, 1120 (1989).
- [9] P. Navrátil, J. P. Vary, and B. R. Barrett, *Phys. Rev. Lett.* **84**, 5728 (2000).
- [10] National Nuclear Data Center, Brookhaven National Laboratory, <http://www.nncd.bnl.gov>.